Comput. Methods Appl. Mech. Engrg. 267 (2013) 261–274

Contents lists available at ScienceDirect

Comput. Methods Appl. Mech. Engrg.

journal homepage: www.elsevier.com/locate/cma

An augmented mixed finite element method for the vorticity–velocity–pressure formulation of the Stokes equations

Verónica Anaya [a], David Mora [a,b,*], Ricardo Ruiz-Baier [c,1]

[a] Departamento de Matemática, Facultad de Ciencias, Universidad del Bío-Bío, Casilla 5-C, Concepción, Chile
[b] Centro de Investigación en Ingeniería Matemática (CI^{2}MA), Universidad de Concepción, Concepción, Chile
[c] Modelling and Scientific Computing, MATHICSE, École Polytechnique Fédérale de Lausanne, CH-1015 Lausanne, Switzerland

ARTICLE INFO

Article history:
Received 4 April 2013
Received in revised form 28 July 2013
Accepted 20 August 2013
Available online 4 September 2013

Keywords:
Stokes equations
Vorticity-based formulation
Mixed finite elements
Error analysis

ABSTRACT

This paper deals with the numerical approximation of the stationary two-dimensional Stokes equations, formulated in terms of vorticity, velocity and pressure, with non-standard boundary conditions. Here, by introducing a Galerkin least-squares term, we end up with a stabilized variational formulation that can be recast as a twofold saddle point problem. We propose two families of mixed finite elements to solve the discrete problem, in the first family, the unknowns are approximated by piecewise continuous and quadratic elements, Brezzi–Douglas–Marini, and piecewise constant finite elements, respectively, while in the second family, the unknowns are approximated by piecewise linear and continuous, Raviart–Thomas, and piecewise constant finite elements, respectively. The wellposedness of the resulting continuous and discrete variational problems are studied employing an extension of the Babuška–Brezzi theory. We establish a priori error estimates in the natural norms, and we finally report some numerical experiments illustrating the behavior of the proposed schemes and confirming our theoretical findings on structured and unstructured meshes. Additional examples of cases not covered by our theory are also presented.

1. Introduction

A fundamental role in a wide range of applied problems is represented by the study of reliable and effective numerical methods to approximate the flow field. In particular, we are interested in the numerical study of the Stokes equations [33]. Numerous stabilization techniques for Stokes and Navier–Stokes problems are available from the literature, tailored for diverse specific applications (see for instance [1,2,11,19,25,36]). We focus our attention on the so-called augmented mixed finite elements, also known as Galerkin least-squares methods [10,12,26], where some terms are added to the variational formulation so that, either the resulting augmented variational formulations are defined by strongly coercive bilinear forms, or they enable to bypass the kernels property, which is very difficult to obtain in practice, or they allow the fulfillment of the inf–sup condition at the continuous and discrete levels in mixed formulations (see also [28]). This approach has been considered in e.g. [5,23,24,29,34,38] for Stokes, generalized Stokes, and Navier–Stokes equations

* Corresponding author at: Departamento de Matemática, Facultad de Ciencias, Universidad del Bío-Bío, Casilla 5-C, Concepción, Chile. Tel.: +56 41 3111146.

E-mail addresses: vanaya@ubiobio.cl (V. Anaya), dmora@ubiobio.cl (D. Mora), ricardo.ruiz@epfl.ch (R. Ruiz-Baier).

[1] Present address: CRET-FGSE, University of Lausanne, UNIL-Mouline, CH-1015, Lausanne, Switzerland.

0045-7825/$ - see front matter
http://dx.doi.org/10.1016/j.cma.2013.08.011

and in [6] for an augmented mixed formulation applied to elliptic problems with mixed boundary conditions, whereas other related methods for the vorticity–velocity–pressure formulation based on least-squares, spectral discretization, hybridizable discontinuous Galerkin, can be found in [4,8,10,16–18,20,39], and the references therein.

Among the available results in the context of mixed finite elements for vorticity-based formulations, we mention the $\mathbb{P}_0 - \mathbb{P}_1 - \mathbb{P}_0$ formulation introduced in [3], and the augmented formulation in [29], written also in terms of stresses ([14,15]). A somewhat different approach has been presented in [22], where the problem is written as a system of first order equations and the resulting variables are discretized in terms of $\mathbb{P}_1 - \mathbb{RT}_0 - \mathbb{P}_0$ elements. In that contribution the authors report optimal convergence for the three fields when structured meshes were employed, whereas on unstructured meshes and in the case of general boundary conditions, the obtained results were inaccurate. In particular, the observed convergence was not optimal, while vorticity and pressure fields were not well approximated, specially on the boundaries. More recently, a stabilization procedure was introduced in [40], mainly to improve the convergence behavior of the method presented in [22]. This strategy is based on adding bubble functions along a part of the boundary. For this scheme, a general theoretical convergence result is provided, but is not optimal. Numerical results shown a better behavior of that scheme for more general boundary conditions.

In this article, we propose, analyze and implement a new stabilized finite element approximation of the Stokes equations, written in terms of the vorticity, velocity, and pressure fields. One of the main goals of the present approach is to improve the convergence properties of the finite element discretization introduced and analyzed in [22] without the need of introducing additional degrees of freedom as in [40], and to build different inf–sup stables families of finite elements to approximate the model problem. This method also exhibits the advantage that the vorticity unknown (which is a sought quantity of practical interest in several industrial applications) can be accessed directly, with the desired accuracy, and without the need of post-processing. This seems to be a quite difficult task in mixed methods written only in terms of vector potential-vorticity (see e.g. [20,32,33]). Our case relates to these methods, however our variational formulation is based on the introduction of a suitable Galerkin least-squares term which lets us analyze the problem directly within the framework developed in e.g. [27,30] (see also [28] for a similar approach applied to the equations of linear elasticity with mixed boundary conditions). The proposed mixed finite element method can be recast as a twofold saddle point problem, and therefore, using an extension of the well-known Babuška-Brezzi theory developed in [27,30], we show that the formulation is well posed and stable in the natural norms. For the numerical approximation, we propose two families of finite elements. In the first one, classical Brezzi–Douglas–Marini finite elements are employed for the velocity field and piecewise constants for the pressure. Since we are interested in accurately recovering the vorticity field, we use a quadratic Lagrange finite element approximation. For the second method, we consider the family introduced in [22], i.e., piecewise linear and continuous finite elements for the vorticity, classical Raviart–Thomas elements for the velocity field and piecewise constants for the pressure. For these methods we prove uniform inf–sup conditions with respect to the discretization parameter h, and the convergence rates are proved to be linear whenever the exact solution of the problem is regular enough. Moreover, numerical experiments with both families of finite elements considered in this paper perform satisfactorily for a variety of boundary conditions and on unstructured meshes without the need of adding additional degrees of freedom. Finally, we stress that the developed framework could be also employed to study other families of finite elements, to analyze the extension to the three-dimensional case, and to study a larger class of nonlinear problems.

1.1. Outline

We have organized the contents of this paper as follows. The remainder of this section introduces some standard notation and needed functional spaces and we describe the boundary value problem of interest and presents the associate dual mixed variational formulation. In Section 2, we introduce the stabilized variational formulation, we provide an abstract framework where our formulation lies, and we prove its unique solvability along with some stability properties. In Section 3 we present two mixed finite element schemes, we provide a stability result and obtain error estimates for the proposed methods. Several numerical results illustrating the convergence behavior predicted by the theory and allowing us to assess the performance of the methods are collected in Section 4.

1.2. Preliminaries

Let Ω be a polygonal Lipschitz bounded domain of $\mathbb{R}^2$ with boundary $\partial\Omega$. For $s \geqslant 0, ||\cdot||_{s,\Omega}$ stands for the norm of the Hilbertian Sobolev spaces $\mathrm{H}^s(\Omega)$ or $\mathrm{H}^s(\Omega)^2$, with the convention $\mathrm{H}^0(\Omega) := \mathrm{L}^2(\Omega)$. We also define for $s \geqslant 0$ the Hilbert space

$$\mathrm{H}^s(\mathrm{div};\Omega) := \left\{ \boldsymbol{v} \in \mathrm{H}^s(\Omega)^n : \ \mathrm{div}\,\boldsymbol{v} \in \mathrm{H}^s(\Omega) \right\},$$

whose norm is given by $\|\boldsymbol{v}\|^2_{\mathrm{H}^s(\mathrm{div};\Omega)} := \|\boldsymbol{v}\|^2_{s,\Omega} + \|\mathrm{div}\,\boldsymbol{v}\|^2_{s,\Omega}$ and denote $\mathrm{H}(\mathrm{div};\Omega) := \mathrm{H}^0(\mathrm{div};\Omega)$.

Moreover, we will denote with c and C, with or without subscripts, tildes, or hats a generic constant independent of the mesh parameter h, which may take different values in different occurrences. In addition, we use the following notation for any vector field $\boldsymbol{v} = (v_i)_{i=1,2}$ and any scalar field θ:

$$\mathrm{div}\ \boldsymbol{v} := \partial_1 v_1 + \partial_2 v_2, \quad \mathrm{rot}\ \boldsymbol{v} := \partial_1 v_2 - \partial_2 v_1,$$
$$\nabla\ \theta := \begin{pmatrix} \partial_1\theta \\ \partial_2\theta \end{pmatrix}, \quad \mathbf{curl}\ \theta := \begin{pmatrix} \partial_2\theta \\ -\partial_1\theta \end{pmatrix}.$$

1.3. Vorticity–velocity–pressure Stokes problem

Let us assume that $\Omega \subset \mathbb{R}^2$ is a bounded and simply connected Lipschitz domain. We denote by $\boldsymbol{n} = (n_i)_{1\leqslant i\leq 2}$ the outward unit normal vector to the boundary $\partial\Omega$ and by $\boldsymbol{t} = (t_i)_{1\leqslant i\leq 2}$ the unit tangent vector to $\partial\Omega$ oriented such that $t_1 = -n_2, t_2 = n_1$. Moreover, we assume that $\partial\Omega$ admits a disjoint partition $\partial\Omega = \Gamma \cup \Sigma$. For the sake of simplicity, we also assume that both Γ and Σ have positive measure.

We are interested in the Stokes problem, formulated in terms of the velocity $\boldsymbol{u}$, the pressure p and the vorticity w of an incompressible viscous fluid (see e.g. [3,21,22,33,40]). Given a force density $\boldsymbol{f}$, vector fields $\boldsymbol{a}$ and $\boldsymbol{b}$, and scalar fields p_0 and w_0, we seek a scalar field w, a vector field $\boldsymbol{u}$ and a scalar field p such that

$$\begin{cases} \nu\ \mathbf{curl}\ w + \nabla p = \boldsymbol{f} \text{ in } \Omega, \\ w - \mathrm{rot}\ \boldsymbol{u} = 0 \text{ in } \Omega, \\ \mathrm{div}\ \boldsymbol{u} = 0 \text{ in } \Omega, \\ \boldsymbol{u}\cdot\boldsymbol{t} = \boldsymbol{a}\cdot\boldsymbol{t} \text{ on } \Sigma, \\ p = p_0 \text{ on } \Sigma, \\ \boldsymbol{u}\cdot\boldsymbol{n} = \boldsymbol{b}\cdot\boldsymbol{n} \text{ on } \Gamma, \\ w = w_0 \text{ on } \Gamma, \end{cases} \tag{1.1}$$

where $\boldsymbol{u}\cdot\boldsymbol{n}$ and $\boldsymbol{u}\cdot\boldsymbol{t}$ stand for the normal and the tangential components of the velocity, respectively. In the model, $\nu > 0$ is the kinematic viscosity of the fluid.

In addition we assume that a *boundary compatibility condition* holds, i.e., there exists a velocity field $\boldsymbol{w} \in \mathrm{L}^2(\Omega)^2$ satisfying $\mathrm{div}\ \boldsymbol{w} = 0$ a.e. in Ω, $\boldsymbol{w}\cdot\boldsymbol{t} = \boldsymbol{a}\cdot\boldsymbol{t}$ on Σ, and $\boldsymbol{w}\cdot\boldsymbol{n} = \boldsymbol{b}\cdot\boldsymbol{n}$ on Γ. For a detailed study on different types of standard and non-standard boundary conditions for incompressible flows we refer to [9,10,35].

For the sake of simplicity, we will work with homogeneous boundary conditions for the normal velocity and for the vorticity, i.e., $\boldsymbol{b} = \mathbf{0}$ and $w_0 = 0$ on Γ.

After testing with adequate functions and imposing the boundary conditions, we obtain the following variational formulation of problem (1.1):

Find $(w, \boldsymbol{u}, p) \in \mathrm{Z}\times\mathrm{H}\times\mathrm{Q}$ *such that*

$$\begin{aligned} &\nu\int_\Omega w\theta - \nu\int_\Omega \mathbf{curl}\ \theta\cdot\boldsymbol{u} = \nu\langle\boldsymbol{a}\cdot\boldsymbol{t},\theta\rangle_\Sigma \quad \forall\theta\in\mathrm{Z}, \\ &-\nu\int_\Omega \mathbf{curl}\ w\cdot\boldsymbol{v} + \int_\Omega p\ \mathrm{div}\ \boldsymbol{v} = -\int_\Omega \boldsymbol{f}\cdot\boldsymbol{v} + \langle\boldsymbol{v}\cdot\boldsymbol{n},p_0\rangle_\Sigma \quad \forall\boldsymbol{v}\in\mathrm{H}, \\ &\int_\Omega q\ \mathrm{div}\ \boldsymbol{u} = 0 \quad \forall q\in\mathrm{Q}, \end{aligned} \tag{1.2}$$

where the spaces above are defined as follows:

$$\mathrm{Z} := \{\theta\in\mathrm{H}^1(\Omega) : \theta = 0 \text{ on } \Gamma\},\ \mathrm{Q} := \mathrm{L}^2(\Omega), \quad \text{and } \mathrm{H} := \{\boldsymbol{v}\in \mathrm{H}(\mathrm{div};\Omega) : \boldsymbol{v}\cdot\boldsymbol{n} = 0 \text{ on } \Gamma\}.$$

We endow each space with the natural norms. Moreover, $\langle\cdot,\cdot\rangle_\Sigma$ denotes the duality pairing between $\mathrm{H}^{1/2}_{00}(\Sigma)'$ and $\mathrm{H}^{1/2}_{00}(\Sigma)$ with respect to the $\mathrm{L}^2(\Sigma)^2$-inner product. We note that because of the boundedness of the normal trace operator $\boldsymbol{v}\mapsto\boldsymbol{v}\cdot\boldsymbol{n}$ from $\mathrm{H}(\mathrm{div};\Omega)$ onto $\mathrm{H}^{-1/2}(\partial\Omega)$ and to the continuity of the restriction operator from $\mathrm{H}^{-1/2}(\partial\Omega)$ to $\mathrm{H}^{1/2}_{00}(\Gamma)'$, we conclude that H is a closed subspace of $\mathrm{H}(\mathrm{div};\Omega)$. (We recall that $\mathrm{H}^{1/2}_{00}(\Gamma)'$ is the dual of $\mathrm{H}^{1/2}_{00}(\Gamma)$, which in its turn is the space of functions from $\mathrm{H}^{1/2}(\Gamma)$ whose extension by zero to the whole boundary $\partial\Omega$ belongs to $\mathrm{H}^{1/2}(\partial\Omega)$).

We stress that the existence and uniqueness of solution to problem (1.2) was proved in [21, Theorem 3].

2. A stabilized mixed formulation of the Stokes problem

2.1. Formulation and preliminary results

In this section, we propose an augmented dual-mixed variational formulation of problem (1.1). We suggest to enrich the mixed variational formulation (1.2) with a residual arising from the first equation of system (1.1). This approach permits us to avoid proving the condition of ellipticity of the bilinear form, defined in (2.5), in the corresponding kernel, which is typically difficult to obtain in this context. Then, we analyze the problem directly under the abstract theory developed in [27,30]. More precisely, we add to the variational problem (1.2) the following Galerkin least-squares term:

$$\kappa \int_\Omega (\nu\,\mathbf{curl}\; w + \nabla p - \boldsymbol{f}) \cdot \mathbf{curl}\;\theta = 0 \quad \forall \theta \in \mathrm{Z}, \tag{2.3}$$

where κ is a positive parameter to be specified later. Using an integration by parts, the fact that div($\mathbf{curl}\;\theta) = 0$, and the boundary condition given in (1.1), we may rewrite (2.3) equivalently as follows:

$$\kappa\nu \int_\Omega \mathbf{curl}\; w \cdot \mathbf{curl}\;\theta = \kappa \int_\Omega \boldsymbol{f} \cdot \mathbf{curl}\;\theta - \kappa\langle \nabla\theta \cdot \boldsymbol{t}, p_0\rangle_\Sigma, \quad \forall \theta \in \mathrm{Z}.$$

In this way, and in addition to (1.2), we propose the following augmented variational formulation:

Find $(w, \boldsymbol{u}, p) \in \mathrm{Z} \times \mathrm{H} \times \mathrm{Q}$ *such that*

$$\begin{aligned} a(w,\theta) + b_1(\theta, \boldsymbol{u}) &= G(\theta) \quad \forall \theta \in \mathrm{Z}, \\ b_1(w, \boldsymbol{v}) + b_2(p, \boldsymbol{v}) &= F(\boldsymbol{v}) \quad \forall \boldsymbol{v} \in \mathrm{H}, \\ b_2(q, \boldsymbol{u}) &= 0 \quad \forall q \in \mathrm{Q}, \end{aligned} \tag{2.4}$$

where the bilinear forms $a : \mathrm{Z} \times \mathrm{Z} \to \mathbb{R}, b_1 : \mathrm{Z} \times \mathrm{H} \to \mathbb{R}, b_2 : \mathrm{Q} \times \mathrm{H} \to \mathbb{R}$, and the linear functionals $G : \mathrm{Z} \to \mathbb{R}$, and $F : \mathrm{H} \to \mathbb{R}$ are defined by

$$a(w,\theta) = \nu \int_\Omega w\theta + \kappa\nu \int_\Omega \mathbf{curl}\; w \cdot \mathbf{curl}\;\theta, \tag{2.5}$$

$$b_1(\theta, \boldsymbol{v}) := -\nu \int_\Omega \mathbf{curl}\;\theta \cdot \boldsymbol{v}, \tag{2.6}$$

$$b_2(q, \boldsymbol{v}) := \int_\Omega q \;\mathrm{div}\; \boldsymbol{v}, \tag{2.7}$$

and

$$G(\theta) := \nu\langle \boldsymbol{a} \cdot \boldsymbol{t}, \theta\rangle_\Sigma + \kappa \int_\Omega \boldsymbol{f} \cdot \mathbf{curl}\;\theta - \kappa\langle \nabla\theta \cdot \boldsymbol{t}, p_0\rangle_\Sigma,$$

$$F(\boldsymbol{v}) := -\int_\Omega \boldsymbol{f} \cdot \boldsymbol{v} + \langle \boldsymbol{v} \cdot \boldsymbol{n}, p_0\rangle_\Sigma,$$

for all $w, \theta \in \mathrm{Z}$, $\boldsymbol{u}, \boldsymbol{v} \in \mathrm{H}$, and $q \in \mathrm{Q}$.

In order to analyze our stabilized variational formulation (2.4), we recall the following results given in [27,30] related to the Babuška–Brezzi theory.

Let Z, H and Q be Hilbert spaces with duals Z', H' and Q', respectively. Consider the following bounded bilinear forms $a : \mathrm{Z} \times \mathrm{Z} \to \mathbb{R}, b_1 : \mathrm{Z} \times \mathrm{H} \to \mathbb{R}, d : \mathrm{H} \times \mathrm{H} \to \mathbb{R}, b_2 : \mathrm{Q} \times \mathrm{H} \to \mathbb{R}$, and the linear functionals $G : \mathrm{Z} \to \mathbb{R}, F : \mathrm{H} \to \mathbb{R}$ and $P : \mathrm{Q} \to \mathbb{R}$. We are interested in the following variational problem: *Given* $(G, F, P) \in \mathrm{Z}' \times \mathrm{H}' \times \mathrm{Q}'$, *find* $(w, \boldsymbol{u}, p) \in \mathrm{Z} \times \mathrm{H} \times \mathrm{Q}$ *such that*

$$\begin{aligned} a(w,\theta) + b_1(\theta, \boldsymbol{u}) &= G(\theta) \quad \forall \theta \in \mathrm{Z}, \\ b_1(w, \boldsymbol{v}) - d(\boldsymbol{u}, \boldsymbol{v}) + b_2(p, \boldsymbol{v}) &= F(\boldsymbol{v}) \quad \forall \boldsymbol{v} \in \mathrm{H}, \\ b_2(q, \boldsymbol{u}) &= P(q) \quad \forall q \in \mathrm{Q}. \end{aligned} \tag{2.8}$$

The following theorem establishes the existence and uniqueness of solution to (2.8).

Theorem 2.1. *Let* $K_2 := \{\boldsymbol{v} \in \mathrm{H} : b_2(q, \boldsymbol{v}) = 0 \quad \forall q \in \mathrm{Q}\}$ *and assume that*

- *There exists* $c_2 > 0$ *such that*

$$\sup_{\substack{\boldsymbol{v} \in \mathrm{H} \\ \boldsymbol{v} \neq 0}} \frac{|\, b_2(q, \boldsymbol{v})\,|}{\|\boldsymbol{v}\|_{\mathrm{H}}} \geqslant c_2 \|q\|_{\mathrm{Q}} \quad \forall q \in \mathrm{Q}.$$

- *There exists* $c_1 > 0$ *such that*

$$\sup_{\substack{\theta \in \mathrm{Z} \\ \theta \neq 0}} \frac{|\, b_1(\theta, \boldsymbol{v})\,|}{\|\theta\|_Z} \geqslant c_1 \|\boldsymbol{v}\|_{\mathrm{H}} \quad \forall \boldsymbol{v} \in K_2.$$

- *The bilinear form* $d(\cdot,\cdot)$ *is positive semi-definite, that is*

$$d(\boldsymbol{v}, \boldsymbol{v}) \geqslant 0 \quad \forall \boldsymbol{v} \in K_2.$$

- *The bilinear form* $a(\cdot,\cdot)$ *is* Z*-elliptic, that is, there exists* $c_3 > 0$ *such that*

$$a(\theta,\theta) \geqslant c_3\|\theta\|_{\mathrm{Z}}^2 \quad \forall \theta \in \mathrm{Z}.$$

Then, for each $(G,F,P) \in \mathrm{Z}' \times \mathrm{H}' \times \mathrm{Q}'$ there exists a unique $(w,\boldsymbol{u},p) \in \mathrm{Z} \times \mathrm{H} \times \mathrm{Q}$ solution of (2.8). Moreover, there exists $C > 0$, depending only on $c_1, c_2, c_3, \|a\|, \|b_1\|, \|b_2\|$ and $\|d\|$ such that

$$\|w\|_{\mathrm{Z}} + \|\boldsymbol{u}\|_{\mathrm{H}} + \|p\|_{\mathrm{Q}} \leqslant C(\|G\|_{\mathrm{Z}'} + \|F\|_{\mathrm{H}'} + \|P\|_{\mathrm{Q}'}).$$

Proof. The result follows from direct application of [30, Theorem 2.1] after noticing that the linear and bounded operator $A : \mathrm{Z} \to \mathrm{Z}'$, induced by the bilinear form $a(\cdot,\cdot)$, is Lipschitz continuous, strongly monotone, and satisfies $A(0) = \mathbf{0}$, thanks to the hypotheses given for $a(\cdot,\cdot)$. □

We will also need the Galerkin approximations of (2.8). To this end, we let $\mathrm{Z}_h, \mathrm{H}_h$ and Q_h be finite dimensional subspaces of Z, H and Q, respectively. Then, the Galerkin scheme associated with (2.8) reads as follows: Find $(w_h, \boldsymbol{u}_h, p_h) \in \mathrm{Z}_h \times \mathrm{H}_h \times \mathrm{Q}_h$ such that

$$\begin{aligned} a(w_h,\theta_h) + b_1(\theta_h,\boldsymbol{u}_h) &= G(\theta_h) \quad \forall \theta_h \in \mathrm{Z}_h,\\ b_1(w_h,\boldsymbol{v}_h) - d(\boldsymbol{u}_h,\boldsymbol{v}_h) + b_2(p_h,\boldsymbol{v}_h) &= F(\boldsymbol{v}_h) \quad \forall \boldsymbol{v}_h \in \mathrm{H}_h,\\ b_2(q_h,\boldsymbol{u}_h) &= P(q_h) \quad \forall q_h \in \mathrm{Q}_h. \end{aligned} \tag{2.9}$$

Now, we also recall the discrete analogue of Theorem 2.1.

Theorem 2.2. *Let $K_{2h} := \{\boldsymbol{v}_h \in \mathrm{H}_h : b_2(q_h,\boldsymbol{v}_h) = 0 \quad \forall q_h \in \mathrm{Q}_h\}$. Assume that*

- *There exists $\bar{c}_2 > 0$ such that*

$$\sup_{\substack{\boldsymbol{v}_h \in \mathrm{H}_h\\ \boldsymbol{v}_h \neq 0}} \frac{|\, b_2(q_h,\boldsymbol{v}_h)\,|}{\|\boldsymbol{v}_h\|_{\mathrm{H}}} \geqslant \bar{c}_2\|q_h\|_{\mathrm{Q}} \quad \forall q_h \in \mathrm{Q}_h.$$

- *There exists $\bar{c}_1 > 0$ such that*

$$\sup_{\substack{\theta_h \in \mathrm{Z}_h\\ \theta_h \neq 0}} \frac{|\, b_1(\theta_h,\boldsymbol{v}_h)\,|}{\|\theta_h\|_{\mathrm{Z}}} \geqslant \bar{c}_1\|\boldsymbol{v}_h\|_{\mathrm{H}} \quad \forall \boldsymbol{v}_h \in K_{2h}.$$

- *The bilinear form $d(\cdot,\cdot)$ is positive semi-definite, that is,*

$$d(\boldsymbol{v}_h,\boldsymbol{v}_h) \geq 0 \quad \forall \boldsymbol{v}_h \in K_{2h}.$$

- *The bilinear form $a(\cdot,\cdot)$ is Z-elliptic, that is, there exists $\bar{c}_3 > 0$ such that*

$$a(\theta,\theta) \geqslant \bar{c}_3\|\theta\|_{\mathrm{Z}}^2 \quad \forall \theta \in \mathrm{Z}.$$

Then, there exists a unique $(w_h,\boldsymbol{u}_h,p_h) \in \mathrm{Z}_h \times \mathrm{H}_h \times \mathrm{Q}_h$ solution of (2.9). Moreover, there exists $\overline{C} > 0$, depending only on $\bar{c}_1, \bar{c}_2, \bar{c}_3, \|a\|, \|b_1\|, \|b_2\|$ and $\|d\|$ such that

$$\|w_h\|_{\mathrm{Z}} + \|\boldsymbol{u}_h\|_{\mathrm{H}} + \|p_h\|_{\mathrm{Q}} \leqslant \overline{C}(\|G_h\|_{\mathrm{Z}_h'} + \|F_h\|_{\mathrm{H}_h'} + \|P_h\|_{\mathrm{Q}_h'}),$$

where $G_h := G|_{\mathrm{Z}_h}, F_h := F|_{\mathrm{H}_h}$ and $P_h := P|_{\mathrm{Q}_h}$.

Proof. See [30, Theorem 3.2]. □

The following theorem establishes the corresponding Céa estimate.

Theorem 2.3. *Let $(w,\boldsymbol{u},p) \in \mathrm{Z} \times \mathrm{H} \times \mathrm{Q}$ and $(w_h,\boldsymbol{u}_h,p_h) \in \mathrm{Z}_h \times \mathrm{H}_h \times \mathrm{Q}_h$ be the unique solution of (2.8) and (2.9), respectively. Then, there exists $\widehat{C} > 0$, independent of h such that*

$$\|w - w_h\|_{\mathrm{Z}} + \|\boldsymbol{u} - \boldsymbol{u}_h\|_{\mathrm{H}} + \|p - p_h\|_{\mathrm{Q}} \leqslant \widehat{C} \inf_{(\theta_h,\boldsymbol{v}_h,q_h) \in \mathrm{Z}_h \times \mathrm{H}_h \times \mathrm{Q}_h} (\|w - \theta_h\|_{\mathrm{Z}} + \|\boldsymbol{u} - \boldsymbol{v}_h\|_{\mathrm{H}} + \|p - q_h\|_{\mathrm{Q}}).$$

Proof. It follows from [30, Theorem 3.3]. □

2.2. Unique solvability of the stabilized formulation

We will now turn to prove that the stabilized variational formulation (2.4) *satisfies the hypotheses of Theorem* 2.1.

Theorem 2.4. *Assume that* $\kappa > 0$, *then problem* (2.4) *admits a unique solution* $(w, \boldsymbol{u}, p) \in \mathrm{Z} \times \mathrm{H} \times \mathrm{Q}$. *Moreover, there exists* $C > 0$ *such that*

$$\|w\|_{1,\Omega} + \|\boldsymbol{u}\|_{\mathrm{H}(div;\Omega)} + \|p\|_{0,\Omega} \leqslant C(\|\boldsymbol{a}\cdot\boldsymbol{t}\|_{-1/2,\Sigma} + \|\boldsymbol{f}\|_{0,\Omega} + \|p_0\|_{1/2,\Sigma}).$$

Proof. It suffices to verify the hypotheses of Theorem 2.1. First, we note that in our case $d = 0$. Moreover, we observe that the bilinear forms a, b_1 and b_2 are bounded. Furthermore, it is well known that the bilinear form b_2 (see (2.7)) satisfies the continuous inf-sup condition on $\mathrm{Q} \times \mathrm{H}$.

We can now characterize the null space of the bilinear form b_2, which is needed to prove the continuous inf-sup condition for the bilinear form b_1 (see (2.6)),

$$K_2 := \{\boldsymbol{v} \in \mathrm{H} : b_2(q, \boldsymbol{v}) = 0 \quad \forall q \in \mathrm{Q}\}, = \{\boldsymbol{v} \in \mathrm{H} : \mathrm{div}\,\boldsymbol{v} = 0 \text{ in } \Omega\}.$$

The next step consists in proving that the bilinear form b_1 satisfies the continuous inf-sup condition on $\mathrm{Z} \times K_2$. Then, given $\boldsymbol{v} \in K_2$, since $\boldsymbol{v}$ is divergence free in Ω, which is simply connected, there exists a scalar function $z \in \mathrm{H}^1(\Omega)$ such that $\boldsymbol{v} = \mathbf{curl}\, z$ in Ω and $z = 0$ on Γ (see e.g. [33]). Therefore, using the Poincaré inequality, we obtain

$$\sup_{\substack{\theta \in \mathrm{Z}\\ \theta \neq 0}} \frac{b_1(\theta, \boldsymbol{v})}{\|\theta\|_{1,\Omega}} \geqslant \frac{b_1(z, \boldsymbol{v})}{\|z\|_{1,\Omega}} \geqslant C_1\|\boldsymbol{v}\|_{0,\Omega} = C_1\|\boldsymbol{v}\|_{\mathrm{H}(\mathrm{div};\Omega)},$$

for all $\boldsymbol{v} \in K_2$, which establishes the continuous inf-sup condition for b_1. Next, we have that the bilinear form a (see (2.5)) is clearly Z-elliptic, in fact, given $\theta \in \mathrm{Z}$ it holds that

$$a(\theta, \theta) = \nu\|\theta\|_{0,\Omega}^2 + \kappa\nu\, |\theta|_{1,\Omega}^2 \geqslant c\|\theta\|_{1,\Omega}^2,$$

where $c = \min\{\nu, \kappa\nu\}$. Finally, the linear functionals F and G are bounded and we have that

$$\|G\|_{\mathrm{Z}'} \leqslant c(\|\boldsymbol{a}\cdot\boldsymbol{t}\|_{-1/2,\Sigma} + \|\boldsymbol{f}\|_{0,\Omega} + \|p_0\|_{1/2,\Sigma})$$

and

$$\|F\|_{\mathrm{H}'} \leqslant c(\|\boldsymbol{f}\|_{0,\Omega} + \|p_0\|_{1/2,\Sigma}),$$

which finishes the proof. □

3. The finite element scheme

In this section we will construct two finite element schemes associated to (2.4), we define explicit finite element subspaces yielding the unique solvability of the discrete schemes, derive the a priori error estimates, and provide the rate of convergence of the methods.

Let $\mathcal{T}_h$ be a regular family of triangulations of the polygonal region $\bar{\Omega}$ by triangles T of diameter h_T with mesh size $h := \max\{h_T : T \in \mathcal{T}_h\}$, and such that there holds $\bar{\Omega} = \cup\{T : T \in \mathcal{T}_h\}$. In addition, given an integer $k \geqslant 0$ and a subset S of $\mathbb{R}^2$, we denote by $\mathbb{P}_k(S)$ the space of polynomials in two variables defined in S of total degree at most k.

We define the following finite element subspaces:

$$\mathrm{Z}_h := \{\theta_h \in \mathrm{Z} : \theta_h|_T \in \mathbb{P}_2(T),\ \forall T \in \mathcal{T}_h\},$$
$$\mathrm{H}_h := \{\boldsymbol{v}_h \in \mathrm{H} : \boldsymbol{v}_h|_T \in \mathbb{P}_1(T)^2,\ \forall T \in \mathcal{T}_h\},$$
$$\mathrm{Q}_h := \{q_h \in \mathrm{Q} : q_h|_T \in \mathbb{P}_0(T),\ \forall T \in \mathcal{T}_h\}.$$

Then, the Galerkin scheme associated with the continuous variational formulation (2.4) reads as follows: *Find* $(w_h, \boldsymbol{u}_h, p_h) \in \mathrm{Z}_h \times \mathrm{H}_h \times \mathrm{Q}_h$ *such that*

$$\begin{aligned} a(w_h, \theta_h) + b_1(\theta_h, \boldsymbol{u}_h) &= G(\theta_h) \quad \forall \theta_h \in \mathrm{Z}_h,\\ b_1(w_h, \boldsymbol{v}_h) + b_2(p_h, \boldsymbol{v}_h) &= F(\boldsymbol{v}_h) \quad \forall \boldsymbol{v}_h \in \mathrm{H}_h,\\ b_2(q_h, \boldsymbol{u}_h) &= 0 \quad \forall q_h \in \mathrm{Q}_h, \end{aligned} \tag{3.10}$$

where $\kappa > 0$ being the same parameter employed in the continuous formulation (2.4).

Throughout the rest of this section, we will show that the discrete variational formulation (3.10) satisfies the hypotheses of Theorem 2.2. With this aim, we recall some notation which will be used in the following.

We introduce the Brezzi–Douglas–Marini interpolation operator $\mathcal{R} : \mathrm{H}^s(\Omega)^2 \cap \mathrm{H} \to \mathrm{H}_h$ for all $s \in (0, 1]$, which is characterized by the identities (see [12]).

$$\int_\ell (\mathcal{R}\boldsymbol{v}\cdot\boldsymbol{n}_\ell)r = \int_\ell (\boldsymbol{v}\cdot\boldsymbol{n}_\ell)r \quad \forall r \in \mathbb{P}_1(\ell)$$

for all edge ℓ of $T \in \mathcal{T}_h$, with $\boldsymbol{n}_\ell$ being a unit normal vector to the edge ℓ.

Let us review some properties of operator $\mathcal{R}$ that we will use in the sequel:

- There exists $c > 0$, independent of h, such that for all $s \in (0,1]$ (see [12])

$$\|\boldsymbol{v} - \mathcal{R}\boldsymbol{v}\|_{\mathrm{H}(\mathrm{div};\Omega)} \leqslant ch^s \|\boldsymbol{v}\|_{\mathrm{H}^s(\mathrm{div};\Omega)}, \tag{3.11}$$

for all $\boldsymbol{v} \in \mathrm{H}^s(\mathrm{div};\Omega) \cap \mathrm{H}$.

Now, for all $s \in (0,1]$, let $\Pi : \mathrm{H}^{1+s}(\Omega) \to \mathrm{Z}_h$ denote the usual Lagrange interpolant. This operator satisfies the following error estimate:

- There exists $c > 0$, independent of h, such that for all $s \in (0,1]$:

$$\|\theta - \Pi\theta\|_{1,\Omega} \leqslant ch^s \|\theta\|_{1+s,\Omega} \quad \forall \theta \in \mathrm{H}^{1+s}(\Omega). \tag{3.12}$$

Let $\mathcal{P}$ be the orthogonal projection from $\mathrm{L}^2(\Omega)$ onto the finite element subspace Q_h, we have that $\mathcal{P}$ satisfies the following error estimate

$$\|q - \mathcal{P}q\|_{0,\Omega} \leqslant Ch^s \|q\|_{s,\Omega} \quad \forall q \in \mathrm{H}^s(\Omega). \tag{3.13}$$

Moreover, the following commuting diagram property holds true:

$$\mathrm{div}\, \mathcal{R}\boldsymbol{v} = \mathcal{P}(\mathrm{div}\boldsymbol{v}) \quad \forall \boldsymbol{v} \in \mathrm{H}^s(\Omega)^2 \cap \mathrm{H}(\mathrm{div};\Omega). \tag{3.14}$$

We are now in a position to establish the unique solvability, and the convergence properties of the discrete problem (3.10).

Theorem 3.1. *Assume that $\kappa > 0$, then problem (3.10) admits a unique solution $(w_h, \boldsymbol{u}_h, p_h) \in \mathrm{Z}_h \times \mathrm{H}_h \times \mathrm{Q}_h$. Moreover, there exists $\widehat{C} > 0$ independent of h such that*

$$\|w - w_h\|_{1,\Omega} + \|\boldsymbol{u} - \boldsymbol{u}_h\|_{\mathrm{H}(\mathrm{div};\Omega)} + \|p - p_h\|_{0,\Omega} \leqslant \widehat{C} \inf_{(\theta_h,\boldsymbol{v}_h,q_h)\in \mathrm{Z}_h\times\mathrm{H}_h\times\mathrm{Q}_h} (\|w - \theta_h\|_{1,\Omega} + \|\boldsymbol{u} - \boldsymbol{v}_h\|_{\mathrm{H}(\mathrm{div};\Omega)} + \|p - q_h\|_{0,\Omega}), \tag{3.15}$$

where $(w, \boldsymbol{u}, p) \in \mathrm{Z} \times \mathrm{H} \times \mathrm{Q}$ is the unique solution to problem (2.4).

Proof. It is enough verified the hypotheses of Theorem 2.2. In fact, it is well known (see [12]) that there exists $\bar{c}_2 > 0$, independent of h such that

$$\sup_{\substack{\boldsymbol{v}_h \in \mathrm{H}_h \\ \boldsymbol{v}_h \neq 0}} \frac{|\, b_2(q_h, \boldsymbol{v}_h)\,|}{\|\boldsymbol{v}_h\|_{\mathrm{H}(\mathrm{div};\Omega)}} \geqslant \bar{c}_2 \|q_h\|_{0,\Omega} \quad \forall q_h \in \mathrm{Q}_h.$$

Now, we characterize the discrete kernel of the bilinear form b_2, which is needed to prove the discrete inf-sup condition for the bilinear form b_1. We have

$$K_{2h} := \{\boldsymbol{v}_h \in \mathrm{H}_h : b_2(q_h, \boldsymbol{v}_h) = 0 \quad \forall q_h \in \mathrm{Q}_h\} = \{\boldsymbol{v}_h \in \mathrm{H}_h : \mathrm{div}\boldsymbol{v}_h = 0 \text{ in } \Omega\}.$$

The next step consists in proving that the bilinear form b_1 satisfies the discrete inf-sup condition on $\mathrm{Z}_h \times K_{2h}$. Then, given $\boldsymbol{v}_h \in K_{2h}$, since $\boldsymbol{v}_h$ is divergence free in Ω, which is simply connected, as in the continuous case, there exists a scalar function $z_h \in \mathrm{H}^1(\Omega)$ such that $\boldsymbol{v}_h = \mathbf{curl}\, z_h$ in Ω and $z_h = 0$ on Γ. Therefore, $z_h|_T \in \mathbb{P}_2(T)$ for all $T \in \mathcal{T}_h$, hence $z_h \in \mathrm{Z}_h$. Thus, using the Poincaré inequality, we have that

$$\sup_{\substack{\theta_h \in \mathrm{Z}_h \\ \theta_h \neq 0}} \frac{b_1(\theta_h, \boldsymbol{v}_h)}{\|\theta_h\|_{1,\Omega}} \geqslant \frac{b_1(z_h, \boldsymbol{v}_h)}{\|z_h\|_{1,\Omega}} \geqslant \bar{c}_1 \|\boldsymbol{v}_h\|_{0,\Omega} = \bar{c}_1 \|\boldsymbol{v}_h\|_{\mathrm{H}(\mathrm{div};\Omega)},$$

for all $\boldsymbol{v}_h \in K_{2h}$, where $\bar{c}_1$ is independent of h, which establishes the discrete inf-sup condition for b_1.

Next, repeating the arguments used in the continuous case, we have that the bilinear form a is clearly Z-elliptic. Finally, estimate (3.15) is a direct consequence of Theorem 2.3, and then the proof is completed. □

The following theorem provides the rate of convergence of our mixed finite element scheme (3.10).

Theorem 3.2. *Let $(w, \boldsymbol{u}, p) \in \mathrm{Z} \times \mathrm{H} \times \mathrm{Q}$ and $(w_h, \boldsymbol{u}_h, p_h) \in \mathrm{Z}_h \times \mathrm{H}_h \times \mathrm{Q}_h$ be the unique solutions to the continuous and discrete problems (2.4) and (3.10), respectively. Assume that $w \in \mathrm{H}^{1+s}(\Omega), \boldsymbol{u} \in \mathrm{H}^s(\Omega)^2, div\, \boldsymbol{u} \in \mathrm{H}^s(\Omega)$ and $p \in \mathrm{H}^s(\Omega)$, for some $s \in (0,1]$. Then, there exists $\widehat{C} > 0$ independent of h such that*

$$\|w - w_h\|_{1,\Omega} + \|\boldsymbol{u} - \boldsymbol{u}_h\|_{\mathrm{H}(div;\Omega)} + \|p - p_h\|_{0,\Omega} \leqslant \widehat{C}h^s(\|w\|_{1+s,\Omega} + \|\boldsymbol{u}\|_{\mathrm{H}^s(div;\Omega)} + \|p\|_{s,\Omega}).$$

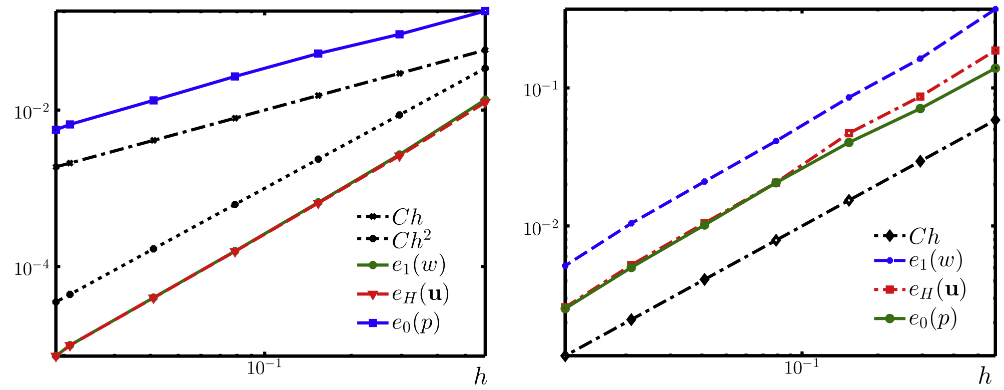

Fig. 1. Example 1: Errors versus the meshsize associated to the mixed FE schemes (3.10) and (3.16) of (1.1) using $\mathbb{P}_2 - \mathbb{BDM}_1 - \mathbb{P}_0$ (left) and $\mathbb{P}_1 - \mathbb{RT}_0 - \mathbb{P}_0$ elements (right). See values in Tables 1, 2.

Proof. The proof follows from (3.15) and standard error estimates for the operators $\mathcal{R}$, Π and $\mathcal{P}$ (see (3.11), (3.12) and (3.13), respectively). $\square$

Remark 1. Let us introduce the local Raviart–Thomas space of order zero

$$\mathbb{RT}_0(T) := \text{span}\left\{\begin{pmatrix}1\\0\end{pmatrix}, \begin{pmatrix}0\\1\end{pmatrix}, \begin{pmatrix}x\\y\end{pmatrix}\right\},$$

where $\begin{pmatrix}x\\y\end{pmatrix}$ is a generic vector of $\mathbb{R}^2$.

Then, we define the following finite element subspaces:

$$\mathcal{Z}_h := \{\theta_h \in \mathrm{Z} : \theta_h|_T \in \mathbb{P}_1(T),\ \forall T \in \mathcal{T}_h\},$$
$$\mathcal{H}_h := \{\boldsymbol{v}_h \in \mathrm{H} : \boldsymbol{v}_h|_T \in \mathbb{RT}_0(T),\ \forall T \in \mathcal{T}_h\},$$
$$\mathcal{Q}_h := \{q_h \in \mathrm{Q} : q_h|_T \in \mathbb{P}_0(T),\ \forall T \in \mathcal{T}_h\},$$

and we introduce the following Galerkin scheme associated with the continuous variational formulation (2.4): *Find* $(w_h, \boldsymbol{u}_h, p_h) \in \mathcal{Z}_h \times \mathcal{H}_h \times \mathcal{Q}_h$ *such that*

$$\begin{aligned} a(w_h, \theta_h) + b_1(\theta_h, \boldsymbol{u}_h) &= G(\theta_h) \quad \forall \theta_h \in \mathcal{Z}_h, \\ b_1(w_h, \boldsymbol{v}_h) + b_2(p_h, \boldsymbol{v}_h) &= F(\boldsymbol{v}_h) \quad \forall \boldsymbol{v}_h \in \mathcal{H}_h, \\ b_2(q_h, \boldsymbol{u}_h) &= 0 \quad \forall q_h \in \mathcal{Q}_h, \end{aligned} \tag{3.16}$$

where $\kappa > 0$ being the same parameter employed in the continuous formulation (2.4). Then, using the arguments considered in this section and the results given in [22], it is easy to prove the following results regarding existence and uniqueness of solution to the discrete scheme (3.16) and the rate of convergence.

Theorem 3.3. *Assume that* $\kappa > 0$, *then problem (3.16) admits a unique solution* $(w_h, \boldsymbol{u}_h, p_h) \in \mathcal{Z}_h \times \mathcal{H}_h \times \mathcal{Q}_h$. *Moreover, assume that* $w \in \mathrm{H}^{1+s}(\Omega), \boldsymbol{u} \in \mathrm{H}^s(\Omega)^2, div\, \boldsymbol{u} \in \mathrm{H}^s(\Omega)$ *and* $p \in \mathrm{H}^s(\Omega)$, *then, there exists* $\widehat{C} > 0$ *independent of h such that*

$$\|w - w_h\|_{1,\Omega} + \|\boldsymbol{u} - \boldsymbol{u}_h\|_{\mathrm{H}(div;\Omega)} + \|p - p_h\|_{0,\Omega} \leqslant \widehat{C} h^s (\|w\|_{1+s,\Omega} + \|\boldsymbol{u}\|_{\mathrm{H}^s(div;\Omega)} + \|p\|_{s,\Omega}).$$

where $(w, \boldsymbol{u}, p) \in \mathrm{Z} \times \mathrm{H} \times \mathrm{Q}$ *is the unique solution to problem (2.4).*

Finally, we stress that our developed framework could be easily adapted to analyze other families of finite elements.

4. Numerical results

In what follows we present three numerical examples using the mixed FE methods described in Section 3, which confirm the theoretical results proved above.

4.1. Example 1: numerical validation

First, we consider a square domain $\Omega = (0, \frac{\pi}{2})^2$, we set $\nu = 0.1, \kappa = 0.01$ and choose suitable source and boundary data $\boldsymbol{f}, \boldsymbol{a}, p_0$ so that the exact solutions of (1.1) are the smooth functions

$$w(x,y) = 2\sin(x)\sin(y), \quad \boldsymbol{u}(x,y) = \begin{pmatrix} \sin(x)\cos(y) \\ -\cos(x)\sin(y) \end{pmatrix}, p(x,y) = (x - \pi/4)^2 + (y - \pi/4)^2,$$

Table 1
Example 1: Convergence history for the stabilized mixed $\mathbb{P}_2 - \mathbb{BDM}_1 - \mathbb{P}_0$ FE approximation of (1.1). Number of mesh nodes, meshsize and errors.

N	h	$e_1(w)$	$r_1(w)$	$e_H(\boldsymbol{u})$	$r_H(\boldsymbol{u})$	$e_0(p)$	$r_0(p)$
27	0.5854	1.3566e-02	-	1.2573e-02	-	1.8466e-01	-
96	0.2945	2.6996e-03	2.3502	2.6033e-03	2.2924	9.3127e-02	0.9966
333	0.1536	6.6007e-04	2.1624	6.4834e-04	2.1343	5.2786e-02	0.8915
1265	0.0789	1.5754e-04	2.1495	1.5612e-04	2.1362	2.6921e-02	1.0103
4972	0.0410	3.9954e-05	2.0993	3.9774e-05	2.0921	1.3304e-02	1.0785
19732	0.0209	9.8486e-06	2.0902	9.8267e-06	2.0868	6.5483e-03	1.0580
27003	0.0188	7.1936e-06	2.0054	7.1798e-06	2.0157	5.6043e-03	1.0911

Table 2
Example 1: Convergence history for the stabilized mixed $\mathbb{P}_1 - \mathbb{RT}_0 - \mathbb{P}_0$ FE approximation of (1.1). Number of mesh nodes, meshsize and errors.

N	h	$e_1(w)$	$r_1(w)$	$e_H(\boldsymbol{u})$	$r_H(\boldsymbol{u})$	$e_0(p)$	$r_0(p)$
27	0.5854	3.7206e-01	-	1.8668e-01	-	1.3879e-01	-
96	0.2945	1.6319e-01	1.1998	8.6598e-02	1.2037	7.0867e-02	0.9786
333	0.1536	8.5384e-02	0.9945	4.7029e-02	0.9953	4.0290e-02	0.8670
1265	0.0789	4.1217e-02	1.0928	2.0609e-02	1.0931	2.0568e-02	1.0088
4972	0.0410	2.0997e-02	1.0320	1.0499e-02	1.0321	1.0167e-02	1.0781
19732	0.0209	1.0445e-02	1.0422	5.2227e-03	1.0422	5.0048e-03	1.0579
77816	0.0114	5.1526e-03	1.1672	2.5763e-03	1.1672	2.5213e-03	1.1324

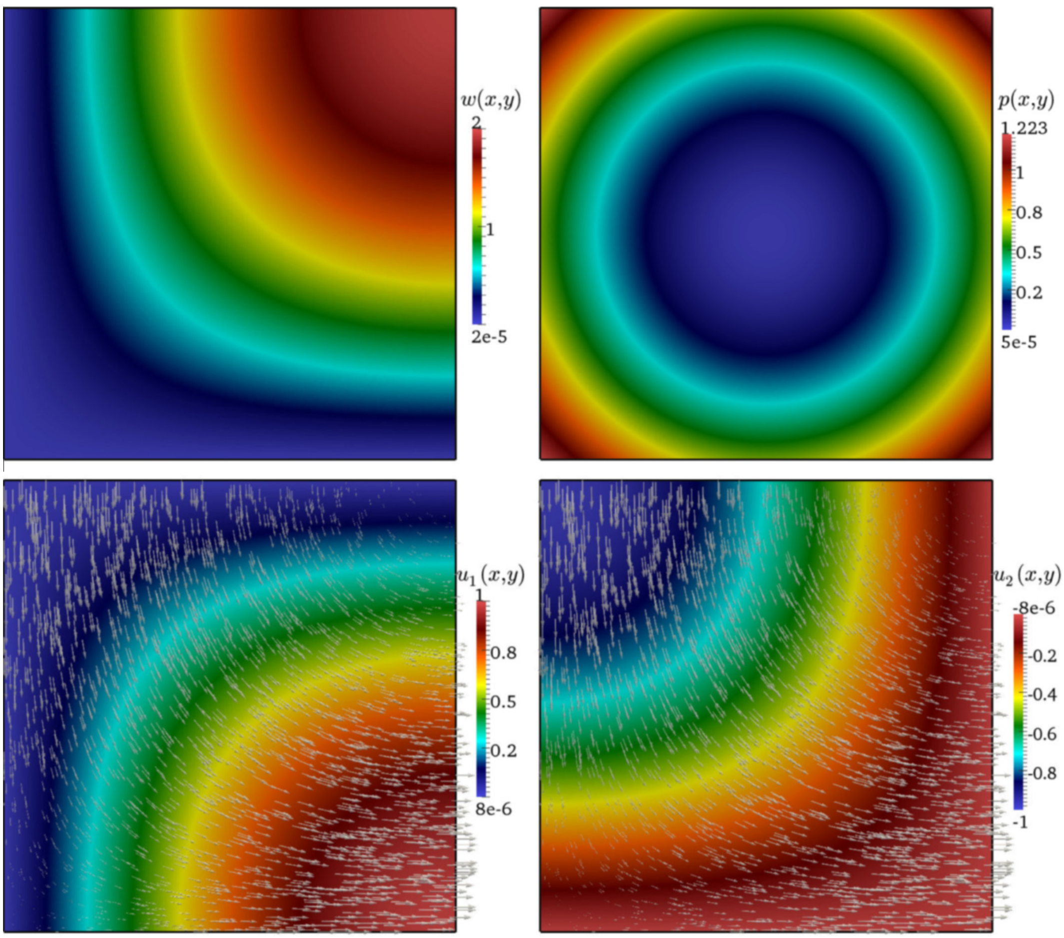

Fig. 2. Example 1: Approximate solutions $w_h, p_h, \boldsymbol{u}_h$ (top left, top right, and bottom, respectively) to (1.1) using the stabilized $\mathbb{P}_2 - \mathbb{BDM}_1 - \mathbb{P}_0$ FE scheme.

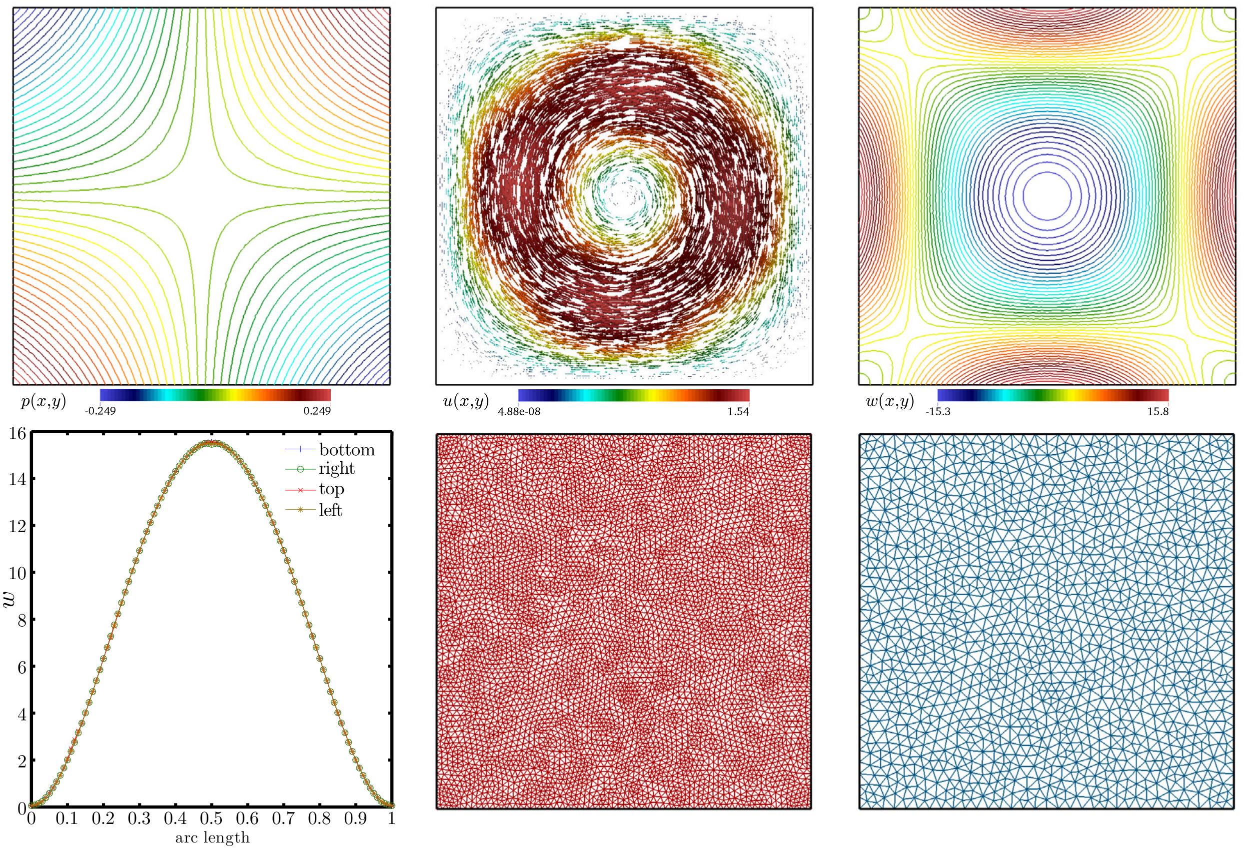

Fig. 3. Example 2: Approximated pressure (top left), velocity field (top middle), vorticity (top left) and vorticity profiles at the four boundaries obtained with a $\mathbb{P}_1 - \mathbb{RT}_0 - \mathbb{P}_0$ method for the Bercovier–Engelman test [7] on an unstructured mesh of 10876 elements (bottom middle). A coarser mesh (one level above of consecutive refinement) is also shown (bottom right).

Table 3
Example 2: Errors versus the meshsize associated to the mixed FE schemes (3.16) and (3.10) for the Bercovier–Engelman problem.

h	$\mathbb{P}_1 - \mathbb{RT}_0 - \mathbb{P}_0$ elements						$\mathbb{P}_2 - \mathbb{BDM}_1 - \mathbb{P}_0$ elements					
	$e_1(w)$	$r_1(w)$	$e_H(\boldsymbol{u})$	$r_H(\boldsymbol{u})$	$e_0(p)$	$r_0(p)$	$e_1(w)$	$r_1(w)$	$e_H(\boldsymbol{u})$	$r_H(\boldsymbol{u})$	$e_0(p)$	$r_0(p)$
0.372678	29.6573	-	0.435655	-	0.544345	-	4.69733	-	0.126246	-	0.0616779	-
0.196419	13.9794	1.17434	0.229679	0.99954	0.147878	2.03476	1.11422	2.24654	0.032461	2.12065	0.0126188	2.47747
0.097754	7.11860	0.96715	0.116195	0.97652	0.038088	1.94395	0.30088	1.87621	0.007986	2.00969	0.0053201	1.23775
0.048108	3.45076	1.02130	0.058540	0.96692	0.010070	1.87632	0.07617	1.93754	0.001939	1.99669	0.0027432	0.93423
0.027913	1.76459	1.23207	0.029647	1.24987	0.002832	2.33041	0.01957	2.49642	0.000500	2.48852	0.0013568	1.29326
0.014244	0.87471	1.04314	0.014491	1.06396	0.000893	1.71515	0.00489	2.05980	0.000123	2.08993	0.0006648	1.06052
0.007291	0.42308	1.08455	0.007248	1.03445	0.000367	1.32837	0.00125	2.01470	0.000032	1.99638	0.0003215	1.04221

satisfying $\mathbf{curl}\, w = 2(\sin(x)\cos(y), \cos(x)\sin(y))^{\mathrm{t}}$, $\nabla p = 2(x - \pi/4, y - \pi/4)^{\mathrm{t}}$, and $\operatorname{div} \boldsymbol{u} = 0$ in Ω. The boundary Σ consists in the top and right sides of the domain, whereas $\Gamma = \partial\Omega \setminus \Sigma$. We construct a nonuniform partition $\mathcal{T}_h$ of Ω and we form a successive refinement $\mathcal{T}_{h'}$ of $\mathcal{T}_h$, where the convergence of the approximate solutions using $\mathbb{P}_2 - \mathbb{BDM}_1 - \mathbb{P}_0$ and $\mathbb{P}_1 - \mathbb{RT}_0 - \mathbb{P}_0$ elements is measured by total and individual errors in the $\mathrm{H}^1(\Omega), \mathrm{H}(\mathrm{div};\Omega)$, and $\mathrm{L}^2(\Omega)$-norms and rates defined as

$$e_1(w) := \|w - w_h\|_{1,\Omega},\; e_H(\boldsymbol{u}) := \|\boldsymbol{u} - \boldsymbol{u}_h\|_{\mathrm{H}(\mathrm{div};\Omega)},$$

$$e_0(p) := \|p - p_h\|_{0,\Omega},\; r_1(w) := \frac{\log(e_1(w)/\hat{e}_1(w))}{\log(h/\hat{h})},$$

$$r_H(\boldsymbol{u}) := \frac{\log(e_H(\boldsymbol{u})/\hat{e}_H(\boldsymbol{u}))}{\log(h/\hat{h})},\; r_0(p) := \frac{\log(e_0(p)/\hat{e}_0(p))}{\log(h/\hat{h})},$$

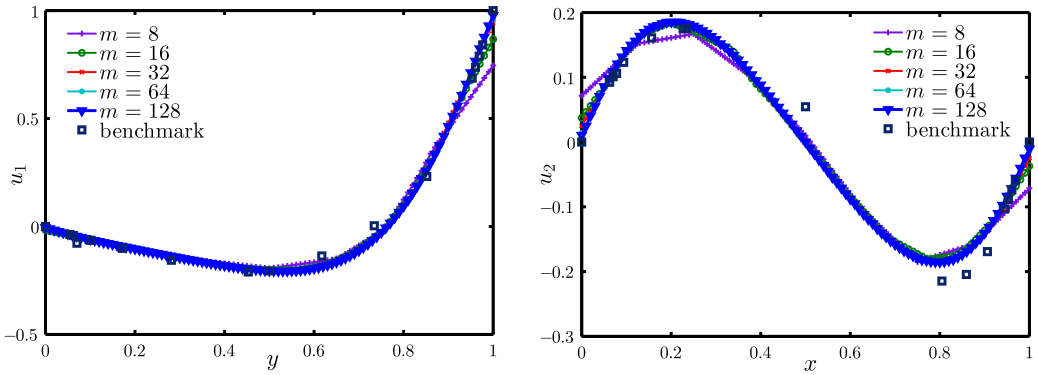

Fig. 4. Example 3: Profiles of velocity components u_1 at $x = 0.5$ (left) and u_2 at $y = 0.5$ (right), for unstructured meshes with m nodes on each side of the domain, and comparison with Navier–Stokes simulations with Re = 100 from [31].

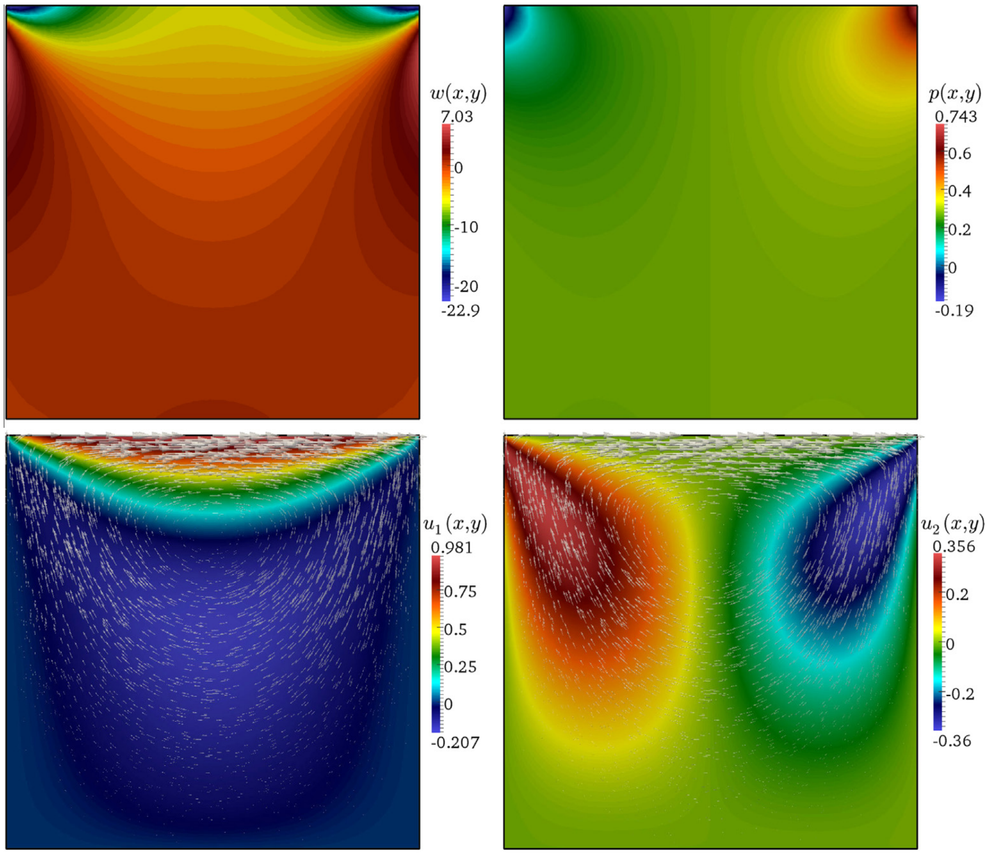

Fig. 5. Example 3: Approximate solutions $w_h, p_h, \boldsymbol{u}_h$ (top left, top right, and bottom, respectively) of the lid-driven cavity test employing a $\mathbb{P}_2 - \mathbb{BDM}_1 - \mathbb{P}_0$ mixed FE method.

where e and $\hat{e}$ denote errors computed on two consecutive meshes of sizes h and $\hat{h}$. These quantities are displayed in Fig. 1 and Tables 1 and 2. For the case of $\mathbb{P}_2 - \mathbb{BDM}_1 - \mathbb{P}_0$ elements, an experimental convergence rate of order h^2 is achieved for the vorticity and for the velocity norms, this fact because the exact solution is smooth in this particular e xample, whereas the pressure norm exhibits an $O(h)$ order of convergence. Experimental convergence rates of order h are observed for all fields when using a $\mathbb{P}_1 - \mathbb{RT}_0 - \mathbb{P}_0$ approximation. These results agree well with the theoretical error estimates from Section 3. The approximate solutions obtained with $\mathbb{P}_2 - \mathbb{BDM}_1 - \mathbb{P}_0$ elements are depicted in Fig. 2.

Our method allows the successful application of boundary conditions of different type as those analyzed here. We present a few of such cases in what follows.

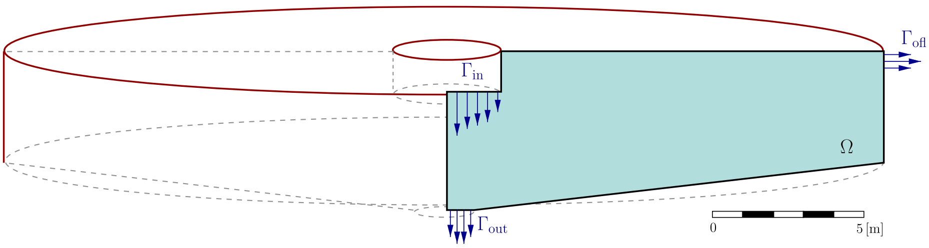

Fig. 6. Example 4: Sketch of the domain and boundaries considered on a section of the secondary settling tank.

Table 4
Example 4: Experimental convergence history for the stabilized mixed $\mathbb{P}_2 - \mathbb{BDM}_1 - \mathbb{P}_0$ FE approximation of the Stokes problem (1.1) on a half-section of a secondary settling unit.

N	h	$e_1(w)$	$r_1(w)$	$e_H(\boldsymbol{u})$	$r_H(\boldsymbol{u})$	$e_0(p)$	$r_0(p)$
451	0.6440	1.4516	-	2.2377e-02	-	1.5722e-01	-
1722	0.3462	0.8449	0.8720	1.3817e-02	0.7781	9.6652e-02	0.7853
3715	0.2424	0.6117	0.9062	9.8126e-03	0.9706	6.9931e-02	0.9105
6543	0.1756	0.4674	0.8348	7.3027e-03	0.8990	5.1902e-02	0.9265
10171	0.1636	0.4389	0.8754	6.9105e-03	0.8835	4.8621e-02	0.9311
14630	0.1228	0.3419	0.8636	5.3044e-03	0.9157	3.7638e-02	0.8968
20534	0.1063	0.3182	0.8957	4.8375e-03	0.9386	2.6829e-02	0.9516
26019	0.0093	0.2657	0.9241	3.7629e-03	0.8853	2.0437e-02	0.8903
32775	0.0083	0.1982	0.9067	2.8171e-03	0.8604	1.7314e-02	0.9463

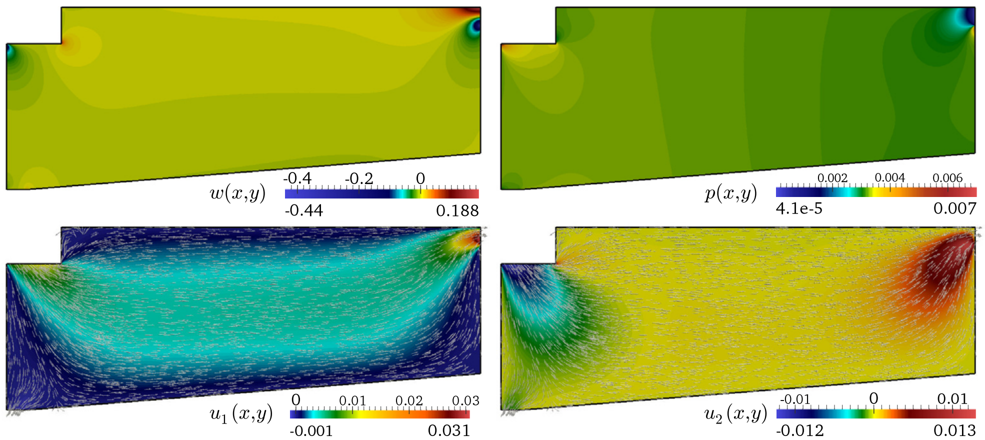

Fig. 7. Example 4: Approximate solutions $w_h, p_h, \boldsymbol{u}_h$ (top left, top right, and bottom, respectively) for the settling tank. The unstructured mesh has 42050 vertices and 84098 triangular elements.

4.2. Example 2: Bercovier–Engelman test case

We perform a second validation test against the well-known Bercovier-Engelman solution [7], and compare the results with those given in [22]. The domain is the unit square $\Omega = (0,1)^2$, and we consider $\Sigma = \partial\Omega$ and $\Gamma = \emptyset$. This implies that the vorticity is not imposed directly at the boundary. We put $\nu = 1, \kappa = 0.01$ and choose suitable source and boundary data $\boldsymbol{f}, \boldsymbol{a}, p_0$ so that the exact solution of (1.1) is

$$w(x,y) = 256[x^2(x-1)^2(6y^2-6y+1) + y^2(y-1)^2(6x^2-6x+1)],$$
$$p(x,y) = (x-1/2)(y-1/2),$$
$$\boldsymbol{u}(x,y) = \begin{pmatrix} -256x^2(x-1)^2y(y-1)(2y-1) \\ -256y^2(y-1)^2x(x-1)(2x-1) \end{pmatrix}.$$

We analyze the convergence properties of the method by considering unstructured meshes as those shown in Fig. 3. As in Example 1, optimal convergence rates are evidenced for all fields in the natural norms when using $\mathbb{P}_1 - \mathbb{RT}_0 - \mathbb{P}_0$ or $\mathbb{P}_2 - \mathbb{BDM}_1 - \mathbb{P}_0$ elements (see Table 3). We stress that for unstructured meshes we obtain accurate results (see Fig. 3).

In particular, we also observe that our approximation retrieves the correct values of the vorticity on the boundaries, which is not necessarily the case in other mixed formulations (see e.g. [22], where also spurious pressure modes are observed when unstructured meshes are employed).

4.3. Example 3: lid-driven cavity

We perform the classical lid-driven cavity benchmark, describing the flow in a container driven by the uniform motion of one lid. The domain is the square $\Omega = (0,1)^2$ discretized on an unstructured mesh with 12139 nodes and 23876 elements. In this case we set $\nu = 0.01, \boldsymbol{f} = \boldsymbol{0}, \kappa = 0.01$ and we impose no slip conditions ($\boldsymbol{u} = \boldsymbol{0}$) on the left, right and bottom boundaries, whereas on the top we put $\boldsymbol{u}\cdot\boldsymbol{t} = \boldsymbol{a}\cdot\boldsymbol{t}$ with $\boldsymbol{a} = (1,0)^{\mathrm{t}}$. Pressure and vorticity fields associated with this type of flow are expected to exhibit corner singularities, that may hinder the convergence of numerical approximations. With our $\mathbb{P}_2 - \mathbb{BDM}_1 - \mathbb{P}_0$ method we obtain discrete fields that remain stable, and corner singularities are satisfactorily resolved, as seen from Fig. 5. This is also observed in Fig. 4, where we display some velocity profiles for successively refined meshes, which are qualitatively and quantitatively comparable to those reported in [9,31].

4.4. Example 4: secondary settling tank

For our last example we assess the applicability of the method in approximating the stationary flow field on a half-section of a secondary settling tank (see [13,37]). A sketch of the domain is depicted in Fig. 6. The inflow, outflow and overflow boundaries $\Gamma_{\mathrm{in}}, \Gamma_{\mathrm{out}}, \Gamma_{\mathrm{ofl}}$ have lengths of 1.5, 0.5 and a 0.5 meters, respectively. A pressure condition with an unknown velocity distribution is imposed on Γ_{ofl} by setting $p = p_{\mathrm{ofl}} = 0$ and $\boldsymbol{u}\cdot\boldsymbol{t} = \boldsymbol{a}\cdot\boldsymbol{t}$ with $\boldsymbol{a} = (0, 1.25\mathrm{e}-4)^{\mathrm{t}}$. A parabolic velocity profile and a compatible vorticity are set on Γ_{in} as $\boldsymbol{u}\cdot\boldsymbol{n} = \boldsymbol{b}_{\mathrm{in}}\cdot\boldsymbol{n}$ with $\boldsymbol{b}_{\mathrm{in}} = (0, 1.25\mathrm{e}-3(x^2-2.25))^{\mathrm{t}}$ and $w = w_{\mathrm{in}} = 0$. On Γ_{out} we apply $\boldsymbol{u}\cdot\boldsymbol{n} = \boldsymbol{b}_{\mathrm{out}}\cdot\boldsymbol{n}$ with $\boldsymbol{b}_{\mathrm{out}} = (0, -1.25\mathrm{e}-4)^{\mathrm{t}}, w = w_{\mathrm{out}} = 0$, and on the remainder of the boundary we impose no-slip data. Since an exact solution is not available, we measure errors by using as a reference solution an approximation computed on a fine mesh (of 93223 vertices and 184972 elements). These errors are reported in Table 4, where we observe that the convergence rates, now slightly below order h for all fields, have deteriorate with respect to those obtained in Examples 1,2. Such a behavior may be explained by the poor regularity of the solutions (associated to the discontinuity of the boundary data for the velocity), and by the non-convexity of the domain. The approximate solutions obtained with $\mathbb{P}_2 - \mathbb{BDM}_1 - \mathbb{P}_0$ finite elements are presented in Fig. 7.

Acknowledgments

The first author was partially supported by CONICYT-Chile through FONDECYT postdoctorado No. 3120197, by project Inserción de Capital Humano Avanzado en la Academia No. 79112012, and DIUBB through project 120808 GI/EF. The second author was partially supported by CONICYT-Chile through FONDECYT project No. 11100180, by DIUBB through project 120808 GI/EF, and Anillo ANANUM, ACT1118, CONICYT (Chile). The third author acknowledges partial support by the ERC advanced grant 227058, project MATHCARD, "Mathematical Modelling and Simulation of the Cardiovascular System". Finally, the authors thank Ricardo Oyarzúa for the fruitful discussions, and two anonymous referees whose suggestions resulted in a number of improvements to the original manuscript.

References

[1] M. Amara, D. Capatina-Papaghiuc, E. Chacón Vera, D. Trujillo, Vorticity–velocity–pressure formulation for Navier–Stokes equations, Comput. Vis. Sci. 6 (2004) 47–52.
[2] M. Amara, D. Capatina-Papaghiuc, D. Trujillo, Stabilized finite element method for Navier–Stokes equations with physical boundary conditions, Math. Comput. 76 (259) (2007) 1195–1217.
[3] M. Amara, E. Chacón Vera, D. Trujillo, Vorticity–velocity–pressure formulation for Stokes problem, Math. Comput. 73 (248) (2004) 1673–1697.
[4] K. Amoura, C. Bernardi, N. Chorfi, Spectral element discretization of the vorticity velocity and pressure formulation of the Stokes problem, M2AN Math. Model. Numer. Anal. 40 (5) (2006) 897–921.
[5] T. Barrios, R. Bustinza, G. García, E. Hernández, On stabilized mixed methods for generalized Stokes problem based on the velocity-pseudostress formulation: a priori error estimates, Comput. Methods Appl. Mech. Engrg. 237/240 (2012) 78–87.
[6] T. Barrios, G.N. Gatica, An augmented mixed finite element method with Lagrange multipliers: a priori and a posteriori error analyses, J. Comput. Appl. Math. 200 (2) (2007) 653–676.
[7] M. Bercovier, M. Engelman, A finite element for the numerical solution of viscous incompressible flows, J. Comput. Phys. 30 (1979) 181–201.
[8] C. Bernardi, N. Chorfi, Spectral discretization of the vorticity, velocity, and pressure formulation of the Stokes problem, SIAM J. Numer. Anal. 44 (2) (2007) 826–850.
[9] P.V. Bochev, Analysis of least-squares finite element methods for the Navier–Stokes equations, SIAM J. Numer. Anal. 34 (5) (1997) 1817–1844.
[10] P.V. Bochev, M.D. Gunzburger, Least-squares finite element Methods, Applied Mathematical Sciences, vol.166, Springer-Verlag, 2009.
[11] F. Brezzi, J. Douglas, Stabilized mixed methods for the Stokes problem, Numer. Math. 53 (1988) 225–235.
[12] F. Brezzi, M. Fortin, Mixed and Hybrid Finite Element Methods, Springer-Verlag, New York, 1991.
[13] R. Bürger, R. Ruiz-Baier, H. Torres, A stabilized finite volume element formulation for sedimentation-consolidation processes, SIAM J. Sci. Comput. 34 (3) (2012) B265–B289.
[14] Z. Cai, C. Tong, P.S. Vassilevski, C. Wang, Mixed finite element methods for incompressible flow: stationary Stokes equations, Numer. Methods Part. Diff. Equ. 26 (4) (2009) 957–978.
[15] Z. Cai, Y. Wang, A multigrid method for the pseudostress formulation of Stokes problems, SIAM J. Sci. Comput. 29 (5) (2007) 2078–2095.
[16] C.L. Chang, A mixed finite element method for the Stokes problem: an acceleration-pressure formulation, Appl. Math. Comput. 36 (2) (1990) 135–146.

[17] C.L. Chang, B.-N. Jiang, An error analysis of least-squares finite element method of velocity–pressure–vorticity formulation for the Stokes problem, Comput. Methods Appl. Mech. Engrg. 84 (3) (1990) 247–255.

[18] B. Cockburn, J. Cui, An analysis of HDG methods for the vorticity–velocity–pressure formulation of the Stokes problem in three dimensions, Math. Comput. 81 (279) (2012) 1355–1368.

[19] J. Douglas, J. Wang, An absolutely stabilized finite element method for the Stokes problem, Math. Comput. 52 (186) (1989) 495–508.

[20] H.-Y. Duan, G.-P. Liang, On the velocity–pressure–vorticity least-squares mixed finite element method for the 3D Stokes equations, SIAM J. Numer. Anal. 41 (6) (2003) 2114–2130.

[21] F. Dubois, Vorticity–velocity–pressure formulation for the Stokes problem, Math. Methods Appl. Sci. 25 (13) (2002) 1091–1119.

[22] F. Dubois, M. Salaün, S. Salmon, First vorticity–velocity–pressure numerical scheme for the Stokes problem, Comput. Methods Appl. Mech. Engrg. 192 (44–46) (2003) 4877–4907.

[23] L.E. Figueroa, G.N. Gatica, N. Heuer, A priori and a posteriori error analysis of an augmented mixed finite element method for incompressible fluid flows, Comput. Methods Appl. Mech. Engrg. 198 (2) (2008) 280–291.

[24] L.E. Figueroa, G.N. Gatica, A. Marquez, Augmented mixed finite element methods for the stationary Stokes equations, SIAM J. Sci. Comput. 31 (2) (2008) 1082–1119.

[25] L.P. Franca, S.L. Frey, Stabilized finite element methods: II. The incompressible Navier–Stokes equations, Comput. Methods Appl. Mech. Engrg. 99 (2-3) (1992) 209–233.

[26] L.P. Franca, T.J.R. Hughes, Two classes of mixed finite element methods, Comput. Methods Appl. Mech. Engrg. 69 (1) (1988) 89–129.

[27] G.N. Gatica, Solvability and Galerkin approximations of a class of nonlinear operator equations, Z. Anal. Anwendungen 21 (3) (2002) 761–781.

[28] G.N. Gatica, Analysis of a new augmented mixed finite element method for linear elasticity allowing $\mathbb{RT}_0 - \mathbb{P}_1 - \mathbb{P}_0$ approximations, M2AN Math. Model. Numer. Anal. 40 (1) (2006) 1–28.

[29] G.N. Gatica, L.F. Gatica, A. Márquez, Augmented mixed finite element methods for a vorticity-based velocity–pressure–stress formulation of the Stokes problem in 2D, Int. J. Numer. Methods Fluids 67 (4) (2011) 450–477.

[30] G.N. Gatica, N. Heuer, S. Meddahi, On the numerical analysis of nonlinear twofold saddle point problems, IMA J. Numer. Anal. 23 (2) (2003) 301–330.

[31] U. Ghia, K.N. Ghia, C.T. Shin, High-Re solutions for incompressible flow using the Navier–Stokes equations and a multigrid method, J. Comput. Phys. 48 (3) (1982) 387–411.

[32] V. Girault, Incompressible finite element methods for Navier–Stokes equations with non-standard boundary conditions in $\mathbb{R}^3$, Math. Comput. 51 (183) (1988) 55–74.

[33] V. Girault, P.A. Raviart, Finite element methods for Navier–Stokes equations, in: Theory and algorithms, Springer-Verlag, Berlin, 1986.

[34] J.J. Heys, E. Lee, T.A. Manteuffel, S.F. McCormick, J.W. Ruge, Enhanced mass conservation in least-squares methods for Navier–Stokes equations, SIAM J. Sci. Comput. 31 (2009) 2303–2321.

[35] B. Jiang, The least-squares finite element method, in: Theory and applications in computational fluid dynamics and electromagnetics, Springer Verlag, Berlin, 1998.

[36] N. Kechkar, D. Silvester, Analysis of locally stabilized mixed finite element methods for the Stokes problem, Math. Comput. 58 (1992) 1–10.

[37] D. Kleine, B.D. Reddy, Finite element analysis of flows in secondary settling tanks, Int. J. Numer. Meth. Engrg. 64 (7) (2005) 849–876.

[38] M. Nickaeen, A. Ouazzi, and S. Turek, Newton multigrid least-squares FEM for the V-V-P formulation of the Navier–Stokes equations, Appl. Math. Report No. 466, TU Dortmund, 2013.

[39] J.P. Pontaza, J.N. Reddy, Spectral/hp least-squares finite element formulation for the Navier–Stokes equations, J. Comput. Phys. 190 (2) (2003) 523–549.

[40] M. Salaün, S. Salmon, Numerical stabilization of the Stokes problem in vorticity–velocity–pressure formulation, Comput. Methods Appl. Mech. Engrg. 196 (9-12) (2007) 1767–1786.